

## Crystal Retro-Engineering: Structural Impact on Silver(I) Complexes with Changing Complexity of Tris(pyrazolyl)methane Ligands

Daniel L. Reger,\* Radu F. Semeniuc, Christine A. Little, and Mark D. Smith

Department of Chemistry and Biochemistry, University of South Carolina, Columbia, South Carolina 29208

Received April 24, 2006

The preparation and structures of seven new silver(I) complexes involving the parent tris(pyrazolyl)methane unit, [C(pz)<sub>3</sub>], as the donor set, {[C<sub>6</sub>H<sub>5</sub>CH<sub>2</sub>OCH<sub>2</sub>C(pz)<sub>3</sub>]Ag}(BF<sub>4</sub>), {[C<sub>6</sub>H<sub>5</sub>CH<sub>2</sub>OCH<sub>2</sub>C(pz)<sub>3</sub>]<sub>2</sub>Ag<sub>3</sub>}(CF<sub>3</sub>SO<sub>3</sub>)<sub>3</sub>, {[HOCH<sub>2</sub>-C(pz)<sub>3</sub>]Ag}(BF<sub>4</sub>), {[HOCH<sub>2</sub>C(pz)<sub>3</sub>]Ag}(CF<sub>3</sub>SO<sub>3</sub>), {[HC(pz)<sub>3</sub>]<sub>2</sub>Ag<sub>2</sub>(CH<sub>3</sub>CN)}(BF<sub>4</sub>)<sub>2</sub>, {[HC(pz)<sub>3</sub>]Ag}(PF<sub>6</sub>), and {[HC(pz)<sub>3</sub>]Ag}(CF<sub>3</sub>SO<sub>3</sub>), are reported. This project is based on a retro-design of our multitopic C<sub>6</sub>H<sub>6-n</sub>[CH<sub>2</sub>OCH<sub>2</sub>C(pz)<sub>3</sub>]<sub>n</sub> (pz = pyrazolyl ring, n = 2, 3, 4, and 6) family of ligands in such a way that each new ligand has one fewer organizational feature. The κ<sup>2</sup>-κ<sup>1</sup> bonding mode of the [C(pz)<sub>3</sub>] units to two silvers, also observed with the multitopic ligands, is the dominant structural feature in all cases. Changing the counterion has important effects on the local structures and on crystal packing. When these structures are compared to similar ones based on the multitopic C<sub>6</sub>H<sub>6-n</sub>[CH<sub>2</sub>OCH<sub>2</sub>C(pz)<sub>3</sub>]<sub>n</sub> ligands, it has been shown that the presence of the rigid parts (central arene core and the [C(pz)<sub>3</sub>] units) are important in order to observe highly organized supramolecular structures. The presence of the flexible ether linkage is also crucial, allowing all noncovalent forces to manifest themselves in a cumulative and complementary manner.

### Introduction

Two important directions have emerged within chemical research around the world: (1) a quest for new materials with promising and useful properties by applying the principles of supramolecular chemistry and (2) a continuous, systematic characterization of the self-assembly processes from a theoretical point of view. While promising results were achieved and startling applications are being developed, much work and effort is still needed in order to lay a foundation for a “grand unified supramolecular theory”.<sup>1</sup>

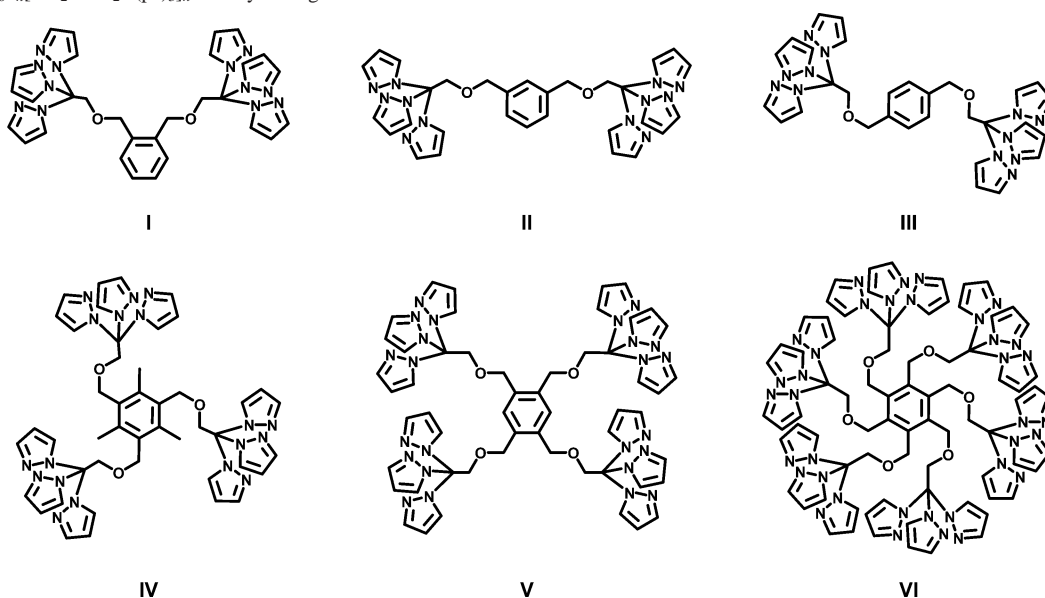
Insight into the self-assembly process can be obtained by carrying out systematic studies using a series of similar complexes assembled from a specific ligand and the same metallic center while imposing subtle alterations in the environment such as changing the anions and the crystallization solvent.<sup>2</sup> Extensive research has been done in this area using mostly rigid ligands because they allow a good prediction of the overall structure, shape, and porosity of the resulting array. The use of rigid ligands is, to some extent, restricting because they limit the structures of possible products and also have to be perfectly tailored to support certain structures. Further, their inherent rigidity hampers the

manifestation of all possible noncovalent forces that can influence the self-assembly process.<sup>3</sup>

Another class of ligands that have been used is the so-called “semi-flexible ligands”, where various donor sets are connected through semi-flexible linkers.<sup>4</sup> The control of their organization is achieved by incorporating within the structures of the building blocks specific recognition sites that will drive the self-assembling process toward the desired

- (1) (a) DeIonno, E.; Tseng, H.-R.; Harvey, D. D.; Stoddart, J. F.; Heath, J. R. *J. Phys. Chem. B* **2006**, *110*, 7609. (b) Moonen, N. N. P.; Flood, A. H.; Fernandez, J. M.; Stoddart, J. F. *Top. Curr. Chem.* **2005**, *262*, 99. (c) Collin, J.-P.; Heitz, V.; Sauvage, J.-P. *Top. Curr. Chem.* **2005**, *262*, 29. (d) Balzani, V.; Credi, A.; Ferrer, B.; Silvi, S.; Venturi, M. *Top. Curr. Chem.* **2005**, *262*, 1. (e) Balzani, V.; Clemente-Leon, M.; Credi, A.; Ferrer, B.; Venturi, M.; Flood, A. H.; Stoddart, J. F. *Proc. Nat. Acad. Sci.* **2006**, *103*, 1178. (f) Saha, S.; Johansson, E.; Flood, A. H.; Tseng, H.-R.; Zink, J. I.; Stoddart, J. F. *Chem. Eur. J.* **2005**, *11*, 6846. (g) Liu, Y.; Flood, A. H.; Bonvallet, P. A.; Vignon, S. A.; Northrop, B. H.; Tseng, H.-R.; Jeppesen, J. O.; Huang, T. J.; Brough, B.; Baller, M.; Magonov, S.; Solares, S. D.; Goddard, W. A.; Ho, C.-M.; Stoddart, J. F. *J. Am. Chem. Soc.* **2005**, *127*, 9745. (h) Badjic, J. D.; Balzani, V.; Credi, A.; Silvi, S.; Stoddart, J. F. *Science* **2004**, *303*, 1845. (i) Hernandez, R.; Tseng, H.-R.; Wong, J. W.; Stoddart, J. F.; Zink, J. I. *J. Am. Chem. Soc.* **2004**, *126*, 3370. (j) Kay, E. R.; Leigh, D. A. *Top. Curr. Chem.* **2005**, *262*, 133. (k) Tian, H.; Wang, Q.-C. *Chem. Soc. Rev.* **2006**, *35*, 361. (l) Yoshizawa, M.; Miyagi, S.; Kawano, M.; Ishiguro, K.; Fujita, M. *J. Am. Chem. Soc.* **2004**, *126*, 9172. (m) Yoshizawa, M.; Takeyama, Y.; Kusakawa, T.; Fujita, M. *Angew. Chem., Int. Ed.* **2002**, *41*, 1347. (n) Fiedler, D.; Bergman, R. G.; Raymond, K. N. *Angew. Chem., Int. Ed.* **2004**, *43*, 6748.

\* To whom correspondence should be addressed. E-mail: Reger@mail.chem.sc.edu.

Chart 1.  $C_6H_{6-n}[CH_2OCH_2C(pz)_3]_n$  Family of Ligands

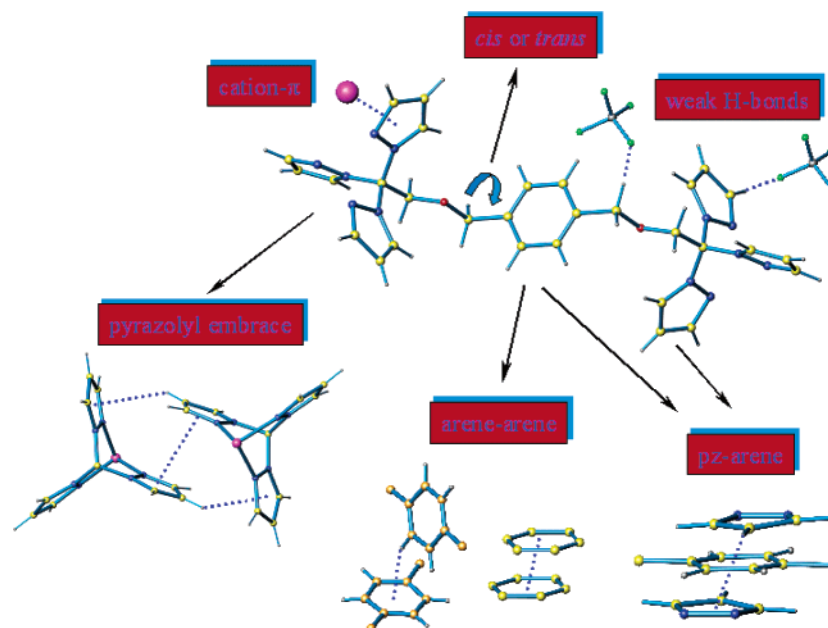
goal.<sup>5</sup> Hydrogen bonding,  $\pi$ - $\pi$  stacking,  $X-H\cdots\pi$  interactions ( $X = O, N, C$ ), and inter-halogen interactions are among the most employed noncovalent forces used to organize a large variety of building blocks (from discrete molecules to coordination polymers) into higher-order supramolecular (not covalently linked) architectures.<sup>6</sup> There are numerous examples where each of these noncovalent interactions was used as the *only* driving force for the organization of the building blocks into supramolecular architectures. In contrast, there are only a few examples where two or more of the aforementioned interactions were *simultaneously* used for the same purposes. A major difficulty in logically using several noncovalent interactions in the same system is the fact that they are not always complementary, making it difficult in most cases to “design” specific architectures.

To study various types of intermolecular forces which may lead to new supramolecular architectures, with the hope of finding complementary noncovalent interactions that would help the researcher designing new solid materials, we have been studying the coordination chemistry of multitopic, semirigid ligands based on poly(pyrazolyl)methane units that contain functionalities suitable to support a variety of weak intermolecular forces. These ligands can adjust their structure to maximize *all* covalent and noncovalent forces within a given system; they are “structurally adaptive”.<sup>7</sup> These ligands are ideal candidates for studying the self-assembly process and the various factors that might have an influence over such processes. One such class is the  $C_6H_{6-n}[CH_2OCH_2C(pz)_3]_n$  ( $n = 2, 3, 4, \text{ and } 6$ ,  $pz =$  pyrazolyl ring) family of ligands, with the structural formulas shown in Chart 1. We have designated these ligands as “third generation” poly-

- (2) (a) Khlobystov, A. N.; Blake, A. J.; Champness, N. R.; Lemenovskii, D. A.; Majouga, G.; Zyk, N. V.; Schroder, M. *Coord. Chem. Rev.* **2001**, *222*, 155. (b) Blake, A. J.; Champness, N. R.; Hubberstey, P.; Li, W. S.; Withersby, M. A.; Schroder, M. *Coord. Chem. Rev.* **1999**, *183*, 117. (c) Blake, A. J.; Baum, G.; Champness, N. R.; Chung, S. S. M.; Cooke, P. A.; Fenske, D.; Khlobystov, A. N.; Lemenovskii, D. A.; Li, W.-S.; Schroder, M. *J. Chem. Soc., Dalton Trans.* **2000**, 4285. (d) Abourahma, H.; Bodwell, G. J.; Lu, J.; Moulton, B.; Pottie, I. R.; Bailey, W. R.; Zaworotko, M. J. *Cryst. Growth Design* **2003**, *3*, 513. (e) Bourne, S. A.; Mondal, A.; Zaworotko, M. J. *Cryst. Eng.* **2001**, *4*, 25. (f) Moulton, Brian; Zaworotko, Michael J. *Chem. Rev.* **2001**, *101*, 1629. (g) Lu, J.; Moulton, B.; Zaworotko, M. J.; Bourne, S. A. *Chem. Commun.* **2001**, 861.
- (3) (a) Yaghi, O. M.; O’Keeffe, M.; Ockwig, N. W.; Chae, H. K.; Eddaoudi, M.; Kim, J. *Nature* **2003**, *423*, 705. (b) Rosi, N. L.; Eckert, J.; Eddaoudi, M.; Vodak, D. T.; Kim, J.; O’Keeffe, M.; Yaghi, O. M. *Science* **2003**, *300*, 1127. (c) Rosi, N. L.; Eddaoudi, M.; Kim, J.; O’Keeffe, M.; Yaghi, O. M. *CrystEngComm* **2002**, *4*, 401. (d) Rosi, N. L.; Eddaoudi, M.; Kim, J.; O’Keeffe, M.; Yaghi, O. M. *Angew. Chem., Int. Ed.* **2002**, *41*, 284. (e) Braun, M. E.; Steffek, C. D.; Kim, J.; Rasmussen, P. G.; Yaghi, O. M. *Chem. Commun.* **2001**, 2532. (f) Eddaoudi, M.; Kim, J.; O’Keeffe, M.; Yaghi, O. M. *J. Am. Chem. Soc.* **2002**, *124*, 376. (g) Eddaoudi, M.; Moler, D. B.; Li, H.; Chen, B.; Reineke, T. M.; O’Keeffe, M.; Yaghi, O. M. *Acc. Chem. Res.* **2001**, *34*, 319. (h) Chen, B.; Eddaoudi, M.; Hyde, S. T.; O’Keeffe, M.; Yaghi, O. M. *Science* **2001**, *291*, 1021. (i) Chen, B.; Eddaoudi, M.; Reineke, T. M.; Kampf, J. W.; O’Keeffe, M.; Yaghi, O. M. *J. Am. Chem. Soc.* **2000**, *122*, 11559. (j) Wang, Y.; Cao, R.; Sun, D.; Bi, W.; Li, X.; Li, X. *J. Mol. Struct.* **2003**, *657*, 301. (k) Zhang, L.-P.; Mak, T. C. W. *Polyhedron* **2003**, *22*, 2787.

- (4) (a) Carlucci, L.; Ciani, G.; Proserpio, D. M.; Rizzato, S. *Chem. Eur. J.* **2002**, *8*, 1519. (b) Carlucci, L.; Ciani, G.; Moret, M.; Proserpio, D. M.; Rizzato, S. *Chem. Mater.* **2002**, *14*, 12. (c) Carlucci, L.; Ciani, G.; Proserpio, D. M.; Rizzato, S. *Chem. Commun.* **2000**, 1319. (d) Carlucci, L.; Ciani, G.; v. Gundenberg, D. W.; Proserpio, D. M. *Inorg. Chem.* **1997**, *36*, 3812. (e) Ng, M. T.; Deivaraj, T. C.; Vittal, J. J. *Inorg. Chim. Acta* **2003**, *348*, 173. (f) Chen, C.-L.; Su, C.-Y.; Cai, Y.-P.; Zhang, H.-X.; Xu, A.-W.; Kang, B.-S. *New Chem.* **2003**, *27*, 790. (g) Gao, E.-Q.; Bai, S.-Q.; Wang, Z.-M.; Yan, C.-H. *J. Chem. Soc., Dalton Trans.* **2003**, 1759. (h) Erxleben, A. *CrystEngComm* **2002**, *4*, 472. (i) Tong, M.-L.; Wu, Y.-M.; Ru, J.; Chen, X.-M.; Chang, H.-C.; Kitagawa, S. *Inorg. Chem.* **2002**, *41*, 4846. (j) Bu, X.-H.; Chen, W.; Hou, W.-F.; Du, M.; Zhang, R.-H.; Brisse, F. *Inorg. Chem.* **2002**, *41*, 3477.
- (5) (a) Brandys, M.-C.; Puddephatt, R. J. *J. Am. Chem. Soc.* **2002**, *124*, 3946. (b) Bu, X.-H.; Chen, W.; Lu, S.-L.; Zhang, R.-H.; Liao, D.-Z.; Bu, W.-M.; Shionoya, M.; Brisse, F.; Ribas, J. *Angew. Chem., Int. Ed.* **2001**, *40*, 3201. (c) McMorran, D. A.; Pfadenhauer, S.; Steel, P. J. *Aust. J. Chem.* **2002**, *55*, 519. (d) Tabellion, F. M.; Seidel, S. R.; Arif, A. M.; Stang, P. J. *J. Am. Chem. Soc.* **2001**, *123*, 11982. (e) Tabellion, F. M.; Seidel, S. R.; Arif, A. M.; Stang, P. J. *J. Am. Chem. Soc.* **2001**, *123*, 7440. (f) Kasai, K.; Aoyagi, M.; Fujita, M. *J. Am. Chem. Soc.* **2000**, *122*, 2140. (g) Seward, C.; Chan, J. L.; Song, D. T.; Wang, S. N. *Inorg. Chem.* **2003**, *42*, 1112. (h) Sun, D. F.; Cao, R.; Sun, Y. Q.; Bi, W. H.; Li, X. H.; Hong, M. C.; Zhao, Y. J. *Eur. J. Inorg. Chem.* **2003**, 38. (i) McMorran, D. A.; Pfadenhauer, S.; Steel, P. J. *Inorg. Chem. Commun.* **2002**, *5*, 449. (j) Fujita, M.; Sasaki, O.; Watanabe, K.; Ogura, K.; Yamaguchi, K. *New J. Chem.* **1998**, *22*, 189.

**Scheme 1.** Ligand  $p\text{-C}_6\text{H}_4[\text{CH}_2\text{OCH}_2\text{C}(\text{pz})_3]_2$  and Possible Noncovalent Interactions That the Ligand Can Promote to Support Supramolecular Structures<sup>a</sup>



<sup>a</sup> Color code: metallic center, purple; carbon, yellow; oxygen, red; nitrogen, blue.

(pyrazolyl)methane ligands. Second generation ligands directly influence the coordination sphere of the metal by placing bulky substituents at the 3-position. Third generation ligands are designed to be those specifically functionalized at the noncoordinating, “back” position of the ligands and can be used to introduce functionality that impacts the supramolecular structure, as well as dictates the directional orientation of multiple  $[\text{C}(\text{pz})_3]$  units in polytopic ligands.<sup>8</sup>

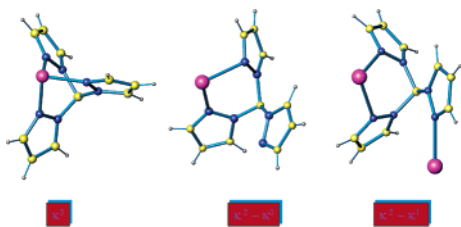
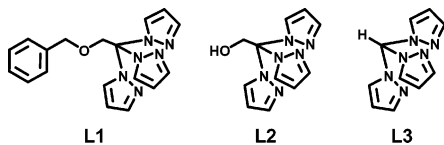
In Scheme 1 we show the noncovalent interactions and/or conformations that have been observed with these ligands, exemplified on the  $p\text{-C}_6\text{H}_4[\text{CH}_2\text{OCH}_2\text{C}(\text{pz})_3]_2$  ligand. The ether linkage offers the possibility of either cis or trans orientations of the sidearms, while the presence of acidic hydrogen atoms on the pyrazolyl ring and methylene groups adjacent to oxygen on the sidearms can promote weak

hydrogen bonds if suitable proton acceptors are introduced into the system.<sup>7a,b,d,h</sup> The pyrazolyl rings and the linking arene ring can act as acceptors in  $\text{C}-\text{H}\cdots\pi$  interactions<sup>7f,g,h</sup> or participate in  $\pi-\pi$  stacking,<sup>7,b,d,f,h</sup> leading to arene–arene, pyrazolyl–arene interactions or the double  $\pi-\pi$  stacking/ $\text{C}-\text{H}\cdots\pi$  interaction that we have named, after a CSD database search showed that it was a general interaction, the “quadruple pyrazolyl embrace”.<sup>7k,l</sup> Another possible noncovalent interaction is cation– $\pi$  contact between a metallic center and a pyrazolyl ring within the ligand.<sup>9</sup> The tris-(pyrazolyl)methane units can also act in different covalent binding modes as (a)  $\kappa^3$  tripodal, (b)  $\kappa^2$  bonded to a single

- (6) (a) Braga, D.; Grepioni, F. *J. Chem. Soc. Dalton Trans.* **1999**, 1. (b) Allen, M. T.; Burrows, A. D.; Mahon, M. F. *J. Chem. Soc., Dalton Trans.* **1999**, 215. (c) Ziener, U.; Breuning, E.; Lehn, J.-M.; Wegelius, E.; Rissanen, K.; Baum, G.; Fenske, D.; Vaughan, G. *Chem. Eur. J.* **2000**, 6, 4132. (d) Goddard, R.; Claramunt, R. M. *Escolastico, C.; Elguero, J. New J. Chem.* **1999**, 23, 237. (e) Calhorda, M. J. *Chem. Commun.* **2000**, 801. (f) Desiraju, G. R. *Acc. Chem. Res.* **1996**, 29, 441. (g) Grepioni, F.; Cojazzi, G.; Draper, S. M.; Scully, N.; Braga, D. *Organometallics*, **1998**, 17, 296. (h) Weiss, H. C.; Boese, R.; Smith, H. L.; Haley, M. M. *Chem. Commun.* **1997**, 2403. (i) Hunter, C. A.; Sanders, J. K. M. *J. Am. Chem. Soc.* **1990**, 112, 5525. (j) Janiak, C. *J. Chem. Soc., Dalton Trans.*, **2000**, 3885 and references therein. (k) Takahashi, H.; Tsuboyama, S.; Umezawa, Y.; Honda, K.; Nishio, M. *Tetrahedron* **2000**, 56, 6185. (l) Tsuzuki, S.; Honda, K.; Uchimaru, T.; Mikami, M.; Tanabe, K. *J. Am. Chem. Soc.* **2000**, 122, 11450. (m) Madhavi, N. N. L.; Katz, A. K.; Carrell, H. L.; Nangia, A.; Desiraju, G. R. *Chem. Commun.* **1997**, 2249. (n) Nishio, M.; Hirota, M.; Umezawa, Y. *The CH/π Interaction Evidence, Nature and Consequences*; Wiley-VCH: New York, 1998. (o) Jennings, W. B.; Farrell, B. M.; Malone, J. F. *Acc. Chem. Res.* **2001**, 34, 885. (p) Reddy, D. S.; Craig, D. C.; Desiraju, G. R. *J. Am. Chem. Soc.* **1996**, 118, 4090. (q) Kowalik, J.; VanDerveer, D.; Clower, C.; Tolbert, L. M. *Chem. Commun.* **1999**, 2007. (r) Freytag, M.; Jones, P. G.; Ahrens, B.; Fischer, A. K. *New J. Chem.* **1999**, 23, 1137. (s) Thaimattam, R.; Reddy, D. S.; Xue, F.; Mak, T. C. W.; Nangia, A.; Desiraju, G. R. *New J. Chem.* **1998**, 22, 143. (t) Edwards, A. J.; Burke, N. J.; Dobson, C. M.; Prout, K.; Heyes, S. J. *J. Am. Chem. Soc.* **1995**, 117, 4637.

- (7) (a) Reger, D. L.; Wright, T. D.; Semeniuc, R. F.; Grattan T. C.; Smith, M. D. *Inorg. Chem.* **2001**, 40, 6212. (b) Reger, D. L.; Semeniuc, R. F.; Smith, M. D. *Inorg. Chem.* **2001**, 40, 6545. (c) Reger, D. L.; Semeniuc, R. F.; Smith, M. D. *Eur. J. Inorg. Chem.* **2002**, 543. (d) Reger, D. L.; Semeniuc, R. F.; Smith, M. D. *J. Chem. Soc., Dalton Trans.* **2002**, 476. (e) Reger, D. L.; Semeniuc, R. F.; Smith, M. D. *Inorg. Chem. Commun.* **2002**, 5, 278. (f) Reger, D. L.; Semeniuc, R. F.; Smith, M. D. *J. Organomet. Chem.* **2003**, 666, 87. (g) Reger, D. L.; Semeniuc, R. F.; Smith, M. D. *J. Chem. Soc., Dalton Trans.* **2003**, 285. (h) Reger, D. L.; Semeniuc, R. F.; Silaghi-Dumitrescu, I.; Smith, M. D. *Inorg. Chem.* **2003**, 42, 3751. (i) Reger, D. L.; Semeniuc, R. F.; Rassolov, V.; Smith, M. D. *Inorg. Chem.* **2004**, 43, 537. (j) Reger, D. L.; Semeniuc, R. F.; Smith, M. D. *Inorg. Chem.* **2003**, 42, 8137. (k) Reger, D. L.; Gardinier, J. R.; Semeniuc, R. F.; Smith, M. D. *J. Chem. Soc., Dalton Trans.*, **2003**, 1712. (l) Reger, D. L.; Semeniuc, R. F.; Gardinier, J. R.; Brown, K. J.; Smith, M. D. In *Functional Nanomaterials*; Geckeler, K. E., Rosenberg, E., Eds.; American Scientific Publishers, 2005; p 411. (8) (a) Reger, D. L.; Gardinier, J. R.; Gemmill, W. R.; Smith, M. D.; Shahin, A. M.; Long, G. J.; Rebbouh, L.; Grandjean, F. *J. Am. Chem. Soc.* **2005**, 127, 2303. (b) Reger, D. L.; Gardinier, J. R.; Smith, M. D.; Shahin, A. M.; Long, G. J.; Rebbouh, L.; Grandjean, F. *Inorg. Chem.* **2005**, 44, 1852. (c) Reger, D. L.; Gardinier, J. R.; Bakbak, S.; Semeniuc, Radu F.; Bunz, U. H. F.; Smith, M. D. *New J. Chem.* **2005**, 29, 1035–1043. (9) For examples of cation– $\pi$  interactions between metallic centers and pyrazolyl rings, see: (a) Craven, E.; Mutlu, E.; Lundberg, D.; Temizdemir, S.; Dechert, S.; Brombacher, H.; Janiak, C. *Polyhedron* **2002**, 21, 553. (b) Kisko, J. L.; Hascall, T.; Kimblin, C.; Parkin, G. *J. Chem. Soc., Dalton Trans.* **1999**, 1929. (c) Janiak, C.; Temizdemir, S.; Scharmann, T. G. *Z. Anorg. Allg. Chem.* **1998**, 624, 755.



**Scheme 2.** Possible Modes of Coordination of Tris(pyrazolyl)methane Units**Chart 2.** Ligands Used in the Present Work

metal with the third pyrazolyl ring not coordinated, and (c)  $\kappa^2-\kappa^1$  bonded bridging two metals (Scheme 2). To date, our most important findings about the self-assembly processes organizing these structures are (a) the ligand usually displays a  $\kappa^2-\kappa^1$  coordination mode of the  $[C(pz)_3]$  units, but the other two coordinating modes were also found in some cases; (b) the “molecular” and supramolecular structures were dependent on the number of sidearms and ligand topology, i.e., the position around the central arene ring of the  $[C(pz)_3]$  units; (c) the overall structures of the crystalline solids showed a dependency on both the counterion and the solvent; and (d) several different anions were involved in weak hydrogen bonds with the metal–organic frameworks. Overall, remarkably intricate topologies have been observed with the metal complexes of these multitopic ligands.

While these findings are clearly helpful in the design of new architectures based on these ligands, three issues still need to be elucidated (1) how important is the organization inherently built into the multitopic ligands by their rigid parts (i.e., directionality of the central arene core and the  $[C(pz)_3]$  units) for the formation of these supramolecular structures; (2) to what extent is the flexibility of the ether linkage (a set of three  $sp^3$  hybridized atoms) responsible for the structurally adaptive nature; and (3) are these two opposed structural characteristics (rigid parts vs flexible linkers) in conflict or are they complementary?

To answer these questions, we started a project based on a retro-design of our multitopic ligands in such a way that each new ligand would have one less organizational feature, as depicted in Chart 2. We have prepared the “one arm” ligand  $C_6H_5CH_2OCH_2C(pz)_3$  (**L1**) to analyze what structural changes in its silver(I) complexes, if any, will occur after such a dramatic modification in ligand topology and topology. We also used the ligand tris-2,2,2-(1-pyrazolyl)ethanol,  $HO-CH_2C(pz)_3$  (**L2**), to assess the influence of the terminal arene core in **L1**. While both of these ligands are “third generation,” the substitution is much less complex than with the multitopic ligands. Finally, we prepared the silver(I) complexes of the “first generation,” parent  $HC(pz)_3$  ligand (**L3**) to evaluate the influence of the flexible, ether-type linker and the rigid arene core in **L1** and our multitopic ligands. We have carefully investigated the supramolecular structural

modifications influenced by several types of noncovalent forces when the anions and crystallization solvent are varied, with an emphasis on the solid-state structures.

## Results

**Syntheses and characterization.** While the ligands **L2** and **L3** were prepared as described in the literature,<sup>10</sup> **L1** was prepared in a one-pot synthesis starting from 1-(bromomethyl)benzene,  $C_6H_5CH_2Br$ , and  $HOCH_2C(pz)_3$  under basic (NaH) conditions. NMR and elemental analysis confirmed its chemical composition and purity. The preparation of complexes of the general formula  $[LAg](counterion)$  was readily achieved by combining the ligands with either  $AgBF_4$ ,  $AgO_3SCF_3$  ( $AgOTf$ ), or  $AgPF_6$ . The compounds (insoluble in halogenated solvents, water, or alcohols but soluble in acetone, acetonitrile, and nitromethane) are white solids that are air stable and show only slight decomposition after several weeks of exposure to daylight. Elemental analyses of the solids correspond to a metal-to-ligand ratio of 1:1. The same metal-to-ligand ratio was found when the starting materials were mixed in different ratios, with the excess starting material recovered from the filtrate. The  $^1H$  NMR spectra of the solids in  $CD_3CN$  show that the acetonitrile completely replaces the ligands in all cases; the spectra of the compounds in  $CD_3CN$  are the same as those of the free ligands in this solvent. However, the  $^1H$  spectra of the compounds in deuterated acetone are clearly different from the free ligands, showing the coordination of the ligands to the silver(I) in solution. Although the X-ray structure shows that the pyrazolyl rings are nonequivalent (vide infra) in the solid state, the NMR spectra show equivalent rings in all cases, presumably because of fast exchange of the ligands and metals on the NMR time scale. This fast exchange process is maintained even at low temperatures. The spectra of metal complexes of the same ligands with different counterions in acetone are essentially identical, showing the same upfield shifts when compared to the free ligand. This result suggests that the cationic species present in acetone solution are identical and anion independent.

**Solid-State Structures.** Crystallization experiments were performed for all compounds by vapor phase diffusion of diethyl ether into an acetone (or, in one case, acetonitrile) solution of the compound. In all but one case, the metal-to-ligand ratio of 1:1 of the initial sample was maintained in the crystalline form. The exception was observed for the crystalline form of the  $AgOTf$  complex of **L1**, where the metal-to-ligand ratio was 3:2.

**Crystal Structure of  $\{[C_6H_5CH_2OCH_2C(pz)_3]Ag\}(BF_4)$  (**1**).** The asymmetric unit of (**1**) $Ag(BF_4)$  consists of five crystallographically independent silver atoms, with  $Ag(1)$  and  $Ag(5)$  located on inversion centers, four **L1** ligands, and four  $BF_4^-$  counterions. All bond lengths and angles fall within the normal range found for these types of compounds.<sup>7</sup> The silver centers in compound **1** show two different geom-

(10) Reger, D. L.; Grattan, T. C.; Brown, K. J.; Little, C. A.; Lamba, J. J. S.; Rheingold, A. L.; Sommer, R. D. *Organomet. Chem.* **2000**, *607*, 120.

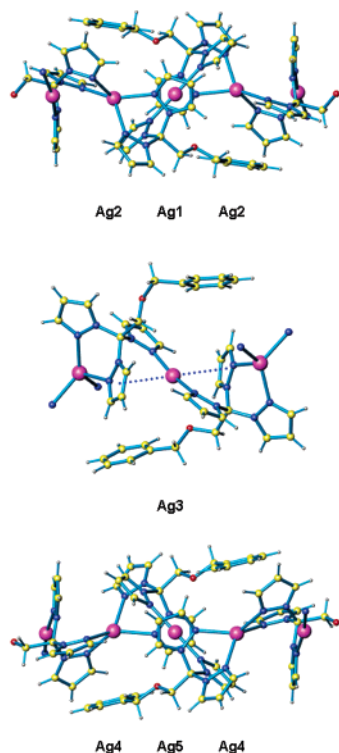


**Figure 1.** Coordination patterns of the ligand and silver environments in  $\{[C_6H_5CH_2OCH_2C(pz)_3]Ag\}(BF_4)_n$  (**1**). Top, linear Ag(1) and tetrahedral Ag(2) coordination; the  $\pi$  sandwich of the pyrazolyl rings around Ag(1) is clearly shown in the middle of the figure. Middle, linear coordination of Ag(3); the cation- $\pi$  contacts are indicated here by the blue dotted lines. Bottom, tetrahedral Ag(4) environment and linear Ag(5) coordination; the cation- $\pi$  contacts for Ag(5) are shown in a similar manner as for Ag(1).

eries: linear, Ag(1), Ag(3), and Ag(5) and tetrahedral, Ag(2) and Ag(4). All **L1** ligands are  $\kappa^2-\kappa^1$  coordinated to the metallic centers. The environment around the Ag(1) and Ag(2) is pictured at the top of Figure 1. Ag(1) is linearly coordinated by two pyrazolyl rings from two different ligands, with the N(131)-Ag(1) distance being 2.104(3) Å with a corresponding angle of 180°. The remaining four pyrazolyl rings from the two tris(pyrazolyl)methane units  $\kappa^1$  bonded to Ag(1), are coordinated to Ag(2) in a  $\kappa^2$  manner, with an average Ag-N distance of 2.3 Å. Furthermore, two pyrazolyl rings coordinated to Ag(2), one from each ligand, are oriented toward Ag(1). Each Ag(1)-centroid distance is 3.18 Å, and the corresponding centroid-Ag(1)-centroid angle is 180°. The pyrazolyl-silver “sandwich”, made up by cation- $\pi$  interactions, is clearly shown in the middle of the top picture in Figure 1. These values are in good agreement with those found for several studies on arene-silver interactions, including statistical analyses based on the existing structures in the Cambridge Structural Database,<sup>11</sup> where distances falling in the range of 2.89–3.37 Å were reported for Ag-arene interactions. Two other **L1** ligands, with two pyrazolyl rings  $\kappa^2$  bonded to the metallic center complete the distorted tetrahedral coordination for the Ag(2) atom.

(11) (a) Mascal, M.; Kerdelhue, J. L.; Blake, A. J.; Cooke, P. A. *Angew. Chem., Int. Ed.* **1999**, *39*, 1968. (b) Mascal, M.; Kerdelhue, J. L.; Blake, A. J.; Cooke, P. A.; Mortimer, R. J.; Teat, S. J. *Eur. J. Inorg. Chem.* **2000**, 485.

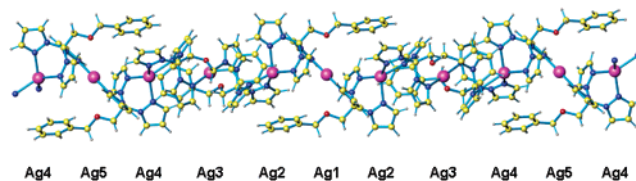


**Figure 2.** Overall 1D strand of **1**. Each Ag(1) is flanked by two Ag(2) and each Ag(5) is flanked by two Ag(4) metallic centers, consistent with their position on inversion centers.

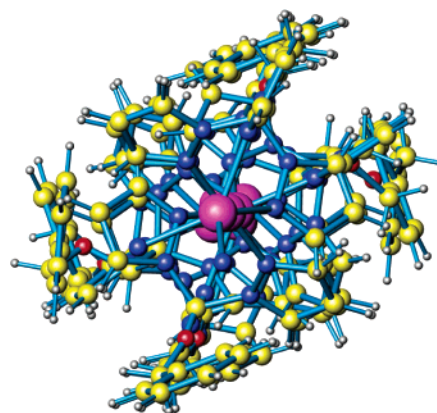


**Figure 3.** View down the chain of **1**. The  $[C(pz)_3Ag]_n$  “argentachains” form a coordination polymer; the  $-CH_2OCH_2C_6H_5$  portion of the ligand is wrapped around the chains.

The remaining pyrazolyl ring from the ligand that completes the coordination around the Ag(2) is bonded to Ag(3), which is the second linear silver, shown in the middle of Figure 1. The other pyrazolyl ring needed for the completion of the linear geometry of the Ag(3) is provided by another ligand, which coordinates again in a  $\kappa^2-\kappa^1$  mode; one pyrazolyl ring coordinates to Ag(3), and the two other are bonded to Ag(4). As with Ag(1), two pyrazolyl rings (one bonded to Ag(2) and one bonded to Ag(4)) are sandwiching the Ag(3) center, as shown in the middle of Figure 3 by the blue dotted lines. Since Ag(3) is not situated on an inversion center, both Ag-N and Ag-centroid distances are not equal. The Ag-N(231) and Ag-N(331) distances are 2.157(3) and 2.169(3) Å, respectively, with a N(231)-Ag(3)-N(331) angle of 168.58(10)°. The Ag- $\pi$  contacts are as follows. Ag(3)-centroid distances are 3.17 and 3.08 Å, respectively, with the corresponding centroid-Ag(3)-centroid angle of 177.6°.

The coordination polymer is further propagated by the  $\kappa^2$  coordination of the remaining pyrazolyl rings from the ligand that is  $\kappa^1$  bonded to Ag(3) and another  $\kappa^2$  bonded ligand to the same Ag(4), as can be seen at the bottom of the Figure 1. As with Ag(2), the environment around Ag(4) is a distorted tetrahedron due to the restricted bite angle of the ligand. The repeating unit of the coordination polymer is completed by the  $\kappa^1$  coordination of the last pyrazolyl ring from the last ligand ( $\kappa^2$  bonded to Ag(4)) to the fifth independent silver within the asymmetric unit, that is Ag(5). The environment around Ag(5) is similar to that of Ag(1) because both of them are situated on inversion centers. The Ag(5)-N(431) distance and the corresponding N(431)-Ag-N(431#1) angle

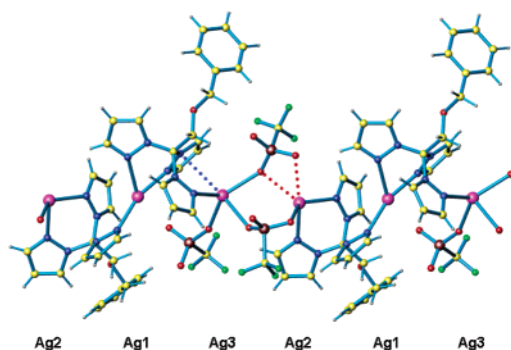


**Figure 4.** Portion of the 1D chain in  $\{[C_6H_5CH_2OCH_2C(pz)_3]_2Ag_3\}(OTf)_3 \cdot 0.5[(CH_3)_2CO]$ .

are 2.131(3) Å and 180°, respectively. Two other pyrazolyl rings are  $\pi$ -coordinated to Ag(5), one from two different ligands. Each Ag(5)–centroid distance is 3.22 Å, and the corresponding centroid–Ag(5)–centroid angle is 180°.

Overall, the structure of **1** is a one-dimensional polymer, as pictured in Figure 2. Each linear Ag(1) and Ag(5) is flanked by two tetrahedral Ag(2) and Ag(4) centers, respectively, which are in turn linked by Ag(3). This  $\kappa^2$ – $\kappa^1$  bridging coordination mode of **L1** create what we call an “argentachain” (no Ag $\cdots$ Ag interactions implied)<sup>12</sup> surrounded by the CH<sub>2</sub>OCH<sub>2</sub>C<sub>6</sub>H<sub>5</sub> coating, Figure 3. The 1D architecture is supported by a series of intrachain C–H $\cdots$  $\pi$  interactions with H–centroid distances ranging from 2.69 to 3.17 Å (perpendicular distances from the H atoms to the ring planes from 2.51 to 2.91 Å) and C–H–centroid angles from 127.1° to 134.2°. The counterions are situated in close proximity of the chains and are “connected” to them by weak C–H $\cdots$ F hydrogen bonds, without expanding the dimensionality of the overall architecture. The C–H $\cdots$ F distances fall in the range 2.13–2.26 Å, and the corresponding C–H–F angles are in the range 159.9–167.8°.

**Crystal Structure of  $\{[C_6H_5CH_2OCH_2C(pz)_3]_2Ag_3\}(OTf)_3 \cdot 0.5[(CH_3)_2CO]$  (**2**·0.5[(CH<sub>3</sub>)<sub>2</sub>CO]).** During the crystallization process of the white powder obtained from the reaction between **L1** and AgOTf, the metal-to-ligand ratio of 1:1 (established on the basis of elemental analysis results) changed to a 3:2 ratio. The compound crystallizes with half a molecule of acetone per unit cell. The structure of (**L1**)<sub>2</sub>Ag<sub>3</sub>(OTf)<sub>3</sub>·0.5[(CH<sub>3</sub>)<sub>2</sub>CO] is a 1D coordination polymer, as with **1**. A portion of the chain is pictured in Figure 4. The structure of **2** shows unique features, not encountered in other cases where the tris(pyrazolyl)methane unit was used as a donor set. There are two ligands, both acting in the bridging  $\kappa^2$ – $\kappa^1$  mode and three silvers, each in different environments: trigonal planar (Ag(1)) with coordination number (C.N.) = 3, trigonal pyramidal (Ag(2)) with C.N. = 3 and distorted tetrahedral (Ag(3)) with C.N. = 4. One ligand is  $\kappa^2$  bonded to Ag(1) and  $\kappa^1$  bonded to Ag(3). The environment around Ag(1) is completed by the second ligand, which is  $\kappa^1$  bonded to the same Ag(1). The Ag(1) atom is in a distorted planar

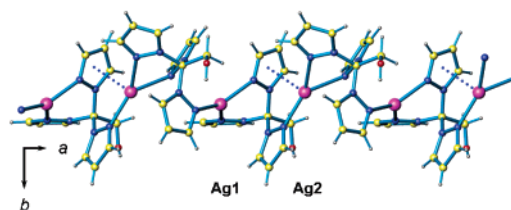


**Figure 5.** 1D chain in  $\{[HOCH_2C(pz)_3]Ag\}(BF_4) \cdot 0.5[(CH_3)_2CO]$  (**3**·0.5[(CH<sub>3</sub>)<sub>2</sub>CO]); the Ag $\cdots$ pz contacts are shown as blue dotted lines.

environment (sum of the N–Ag(1)–N bond angles = 357.26°), with a significant distortion caused by the restricted angle [78.12(12)°] of the  $\kappa^2$  bonded ligand. There are no other contacts for this Ag(1) atom, the two pyrazolyl rings oriented toward the Ag(1), shown at the right side of the figure are too far away to consider a cation– $\pi$  interaction between the two moieties. The Ag(2) is coordinated by two pyrazolyl rings from the second ligand and one triflate anion in a nonplanar arrangement. If we consider two other Ag–O contacts, of 2.61 and 2.75 Å, indicated by two red dotted lines in Figure 4, the polyhedron around Ag(2) becomes a trigonal bipyramid. The Ag(3) center is  $\kappa^1$  coordinated by the remaining pyrazolyl ring from the first ligand and by all three triflate counterions. The nitrogen atom from the pyrazolyl ring and two oxygen atoms from two different anions form the base of a trigonal pyramid and a third oxygen, coming from one triflate counterion, completes the pyramid. The silver(I) center is positioned within the base, the sum of N–Ag–O and O–Ag–O bond angles = 359.48°. One pyrazolyl ring from the pair that chelates the Ag(1) atom is oriented toward the Ag(3) atom, making a cation– $\pi$  contact, at 3.00 Å, as is indicated by the blue dotted line in Figure 4. Considering this interaction, the geometry around the silver(I) center becomes trigonal bipyramidal, with three short bonds in the equatorial plane and two long bonds in the axial plane. The repeating unit of **2** is best described as “independent” (**L1**)<sub>2</sub>(Ag)<sub>3</sub> units linked by two triflate anions into argentachains through covalent and secondary bonds. With no other noncovalent interactions being identified, the remaining crystal packing of **2** is based solely on van der Waals forces.

**Crystal Structure of  $\{[HOCH_2C(pz)_3]Ag\}(BF_4) \cdot 0.5[(CH_3)_2CO]$  (**3**·0.5[(CH<sub>3</sub>)<sub>2</sub>CO]).** Crystallization of the white powder from an acetone–diethyl ether system produced a 1D coordination polymer made up by the  $\kappa^2$ – $\kappa^1$  bonding mode of the [C(pz)<sub>3</sub>] unit, as pictured in Figure 5. The asymmetric unit contains two independent silver atoms, two **L2** ligands, two BF<sub>4</sub><sup>–</sup> counterions, and an acetone molecule of crystallization. Both silver(I) centers are found alternatively situated within the same chain and each  $\kappa^2$  bonded by one of the ligands and  $\kappa^1$  bonded by the second **L2**. Both the Ag(1) and Ag(2) environments are trigonal planar, with the sum of the corresponding N–Ag–N bond angles being 359.67° and 359.68°, respectively. The difference between Ag(1) and Ag(2) is that Ag(2) is involved in a cation– $\pi$  interaction with one of the pyrazolyl rings from the pair that is  $\kappa^2$  bonded to Ag(1), as shown by the blue dotted lines in Figure 5.

(12) We use the term “argentachain” to describe the –AgNCCNN– sequence of atoms that form the coordination polymer, created by the  $\kappa^2$ – $\kappa^1$  coordination mode of the tris(pyrazolyl)methane donor set without claiming Ag–Ag contacts of any kind; see also ref 7g.



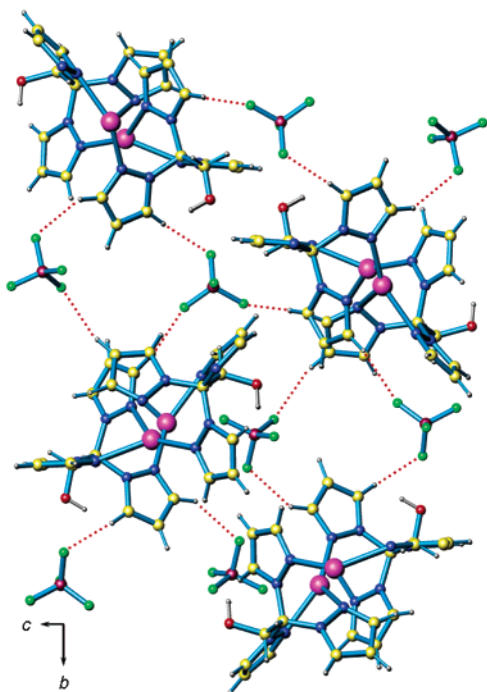


**Figure 6.** Crystal packing in  $3 \cdot 0.5[(\text{CH}_3)_2\text{CO}]$  oriented down the argentachains; the  $\text{C}-\text{H}\cdots\text{F}$  hydrogen bonds are shown as red dotted lines.

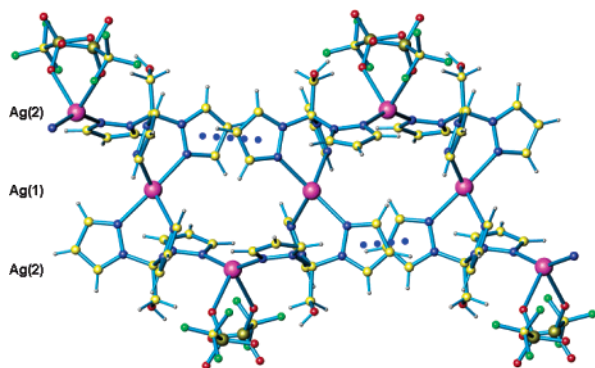


**Figure 7.** Structure of  $[\text{HOCH}_2\text{C}(\text{pz})_3]\text{Ag}(\text{OTf})$  (**4**); the  $\pi-\pi$  stacking component of the pyrazolyl embrace interaction is shown as blue dotted lines.

The crystal packing of  $3 \cdot 0.5[(\text{CH}_3)_2\text{CO}]$  (Figure 6) is dominated by a network of  $\text{C}-\text{H}\cdots\text{F}$  hydrogen bonds, shown in Figure 6 by the red dotted lines. There are two  $\text{BF}_4^-$  anions within the asymmetric unit, each with different supramolecular contacts but both having the same function: connecting the covalent 1D cationic strands into a 3D architecture. The average  $\text{H}\cdots\text{F}$  distance is 2.41 Å, and the average  $\text{C}-\text{H}-\text{F}$  angle is 164.2°. The  $-\text{CH}_2\text{OH}$  groups of each ligand were both found to be disordered over two orientations, and therefore, their contribution to the crystal packing is difficult to interpret.

**Crystal Structure of  $[\text{HOCH}_2\text{C}(\text{pz})_3]\text{Ag}(\text{OTf})$  (**4**).** The change in counterion from  $\text{BF}_4^-$  to  $\text{OTf}^-$  generated major structural changes of the cationic 1D strand, pictured in Figure 7. There are two crystallographically inequivalent Ag cations, both having a distorted tetrahedral coordination. The Ag(1) atoms are coordinated by two pairs of pyrazolyl rings from two different ligands, while Ag(2) atoms are coordi-

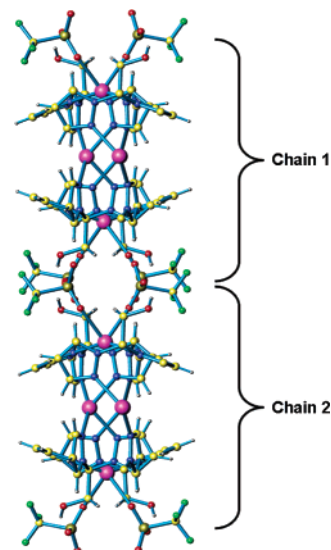


**Figure 8.** Sheet formation in **4** shown down the argentachains pictured in Figure 7.

nated by the remaining two pyrazolyl rings and two triflate counterions. The sinusoidal arrangement of these strands is supported by a “pyrazolyl embrace” interaction forming metalocycles along the strand. This interaction is a concerted set of noncovalent interactions between a pyrazolyl tetrad, consisting of cooperative  $\pi-\pi$  and two  $\text{C}-\text{H}\cdots\pi$  interactions.<sup>7k,1</sup> In **4**, two of the pyrazolyl rings that chelate the Ag(1) atoms are  $\pi$ -stacked at a perpendicular distance between the planes of 3.6 Å, as pointed out in Figure 7 by the blue dotted lines, with a slip angle of 22.8°. The hydrogen atoms from the 4-position of the rings involved in the  $\pi-\pi$  stacking interaction are oriented toward the other two pyrazolyl rings that are coordinated to Ag(1), with a  $\text{H}-\text{centroid}$  distance of 3.2 Å ( $\text{C}-\text{centroid}$  distance of 4.1 Å) and a  $\text{C}-\text{H}-\text{centroid}$  angle of 146.9°. Another interaction that supports the 1D coordination polymer is an intrachain hydrogen bond, involving the terminal OH group of the ligand. The hydrogen atoms are oriented toward the oxygen atoms from the triflate groups, with the  $\text{H}\cdots\text{O}$  distance = 2.29 Å, the  $\text{O}\cdots\text{O}$  distance = 3.04 Å, and the  $\text{O}-\text{H}-\text{O}$  angle = 150.5°.

The chains are arranged into sheets (Figure 8) by two  $\text{C}-\text{H}\cdots\text{O}$  interactions. Two hydrogen atoms H(11) and H(21) situated at the 3-position of the pyrazolyl rings are oriented toward two different oxygen atoms from the triflate groups. The geometric parameters for these two interactions are as follows. The  $\text{H}\cdots\text{O}$  distances are for both interactions 2.38 Å, with only the  $\text{C}-\text{H}-\text{O}$  angles and  $\text{C}\cdots\text{O}$  separations being different, 169.89° and 147.41°, respectively, and 3.32 and 3.22 Å, respectively.

**Crystal Structure of  $[\text{HC}(\text{pz})_3]_2\text{Ag}_2(\text{CH}_3\text{CN})\{\text{BF}_4\}_2$  (**5**).** Crystals suitable for X-ray diffraction studies were obtained from an acetonitrile–diethyl ether system (efforts to grow crystals from the acetone–diethyl ether were unsuccessful). Although the ligand-to-metal ratio is 1:1, the asymmetric unit contains two chemically identical but crystallographically inequivalent **L3** ligands, two Ag centers, one coordinated  $\text{CH}_3\text{CN}$  molecule, and two  $\text{BF}_4^-$  counter-

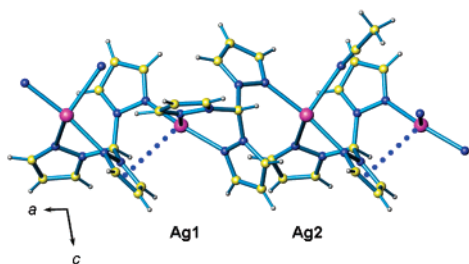


**Figure 9.** 1D chain in  $\{[\text{HC}(\text{pz})_3]_2\text{Ag}_2(\text{CH}_3\text{CN})\}(\text{BF}_4)_2$  (**5**); the  $\text{Ag}\cdots\text{pz}$  contacts are shown as blue dotted lines.

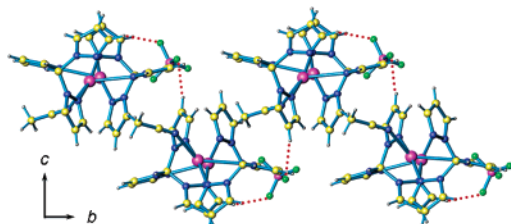


**Figure 10.** One corrugated sheet in **5**, viewed down the argentachains; the  $\text{C}-\text{H}\cdots\text{F}$  hydrogen bonds are shown as red dotted lines.

ions. The covalent 1D argentachain of **5** is built up by the same  $\kappa^2-\kappa^1$  coordination mode of the ligands to both silver centers. However, the covalent and noncovalent silver environments within the strand are different for the two **L3**–Ag pairs. As seen in Figure 9, Ag(1) is into an almost planar environment, the sum of the corresponding N–Ag–N bond angles being  $358.58^\circ$ , the metallic center being slightly out of the plane defined by the three nitrogen atoms. In addition, there is a cation– $\pi$  interaction between the silver(I) center and one of the pyrazolyl rings from the ligand that is  $\kappa^2$  bonded to Ag(2), pictured in Figure 9 by the blue dotted line. The  $\text{Ag}\cdots$ centroid distance is 3.17 Å, with a perpendicular distance from Ag to the pyrazolyl ring of 2.9 Å. The Ag(2) atom is four coordinate, bonded to the three pyrazolyl rings coming from two **L3** ligands and an acetonitrile molecule. If we consider only the pyrazolyl rings, the  $\text{AgN}_3$  core is a flattened trigonal pyramid, the sum of the corresponding N–Ag–N bond angles being  $353^\circ$ . Together with the acetonitrile molecule, the Ag(2) environment is a highly distorted tetrahedron.

The  $\text{BF}_4^-$  counterions are situated along the chain. The shortest Ag(1)–F and Ag(2)–F distances are 3.18 and 3.00 Å, respectively, too long to be considered  $\text{Ag}\cdots\text{F}$  contacts. However, there are several (C)H $\cdots$ F hydrogen bonds, involving both anions. For the first  $\text{BF}_4^-$  group, the average H $\cdots$ F distance is 2.39 Å, with a corresponding average C–H–F angle of  $154.8^\circ$ . The second  $\text{BF}_4^-$  group was found disordered over two orientations; therefore, an accurate analysis of its contribution to the crystal packing is precluded. Considering only the interactions of the well-behaved  $\text{BF}_4^-$  moiety, shown as red dotted lines in Figure 10, the one-dimensional strands are organized in corrugated sheets in the *ab* plane of the unit cell.

**Crystal Structure of  $\{[\text{HC}(\text{pz})_3]\text{Ag}\}(\text{PF}_6)\cdot 0.5[(\text{CH}_3)_2\text{CO}]$  (**2**·**0.5** $[(\text{CH}_3)_2\text{CO}]$ ).** Similar to **5**, with  $\text{PF}_6^-$  as the anion, the resulting structure is again a simple coordination polymer built up by the same  $\kappa^2-\kappa^1$  bonding mode of the ligand,

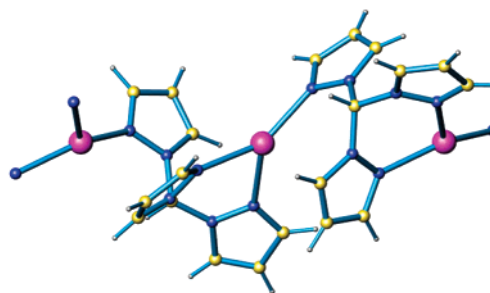


**Figure 11.** 1D chain in  $\{[\text{HC}(\text{pz})_3]\text{Ag}\}(\text{PF}_6)\cdot 0.5[(\text{CH}_3)_2\text{CO}]$ ; no inter- or intrastrand contacts were observed.

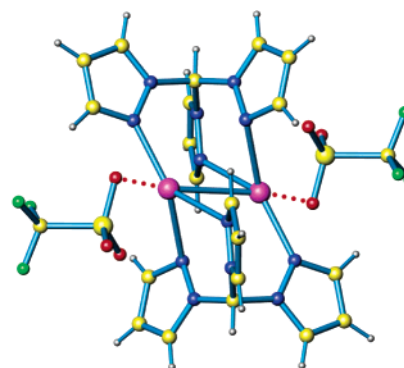


**Figure 12.** Structural characteristics of the bimetallic unit in  $\{[\text{HC}(\text{pz})_3]_2\text{Ag}_2\}(\text{OTf})_2$ ;  $\text{Ag}\cdots$ oxygen contacts are shown as red dotted lines.

Figure 11. In contrast to **5**, a check of the supramolecular structure revealed *no association* between the 1D strands of the coordination polymer or between the strands and the acetone molecule of crystallization.

**Crystal Structure of  $\{[\text{HC}(\text{pz})_3]_2\text{Ag}_2\}(\text{OTf})_2$  (**7**).** The change in counterion from either  $\text{BF}_4^-$  or  $\text{PF}_6^-$  to  $\text{F}_3\text{CSO}_3^-$  generated dramatic changes in the molecular and crystal structure of the compound. Crystallization from an acetone–diethyl ether system produced a discrete bimetallic compound, rather than a coordination polymer, see Figure 12. Although the ligand-to-metal ratio is still 1:1, the compound is a dimer, built up by the two **L3** ligands  $\kappa^2-\kappa^1$  bonding to the same two silvers. Each ligand chelates a different silver using two pyrazolyl rings, while the third ring has  $\kappa^1$  bonding to the silver  $\kappa^2$  bonded to the other ligand. The distance between the silver atoms is 2.86 Å, considerably shorter than the sum of silver–silver van der Waals radii (3.44 Å),<sup>13</sup> which is indicative of a strong Ag–Ag interaction. Such interactions have been shown to influence the outcome of several supramolecular assemblies, and their importance has been crystallographically and theoretically documented.<sup>14</sup> Each silver is equatorially surrounded by three nitrogen atoms. The sum of Ag–N angles around the silver is  $358.54^\circ$ , thus placing it in a slightly distorted trigonal planar geometry. In addition, the triflate counterions are in close proximity to the metallic centers, with one Ag–O distance = 2.82 Å. If

(13) Bondi, A. *J. Phys. Chem.* **1964**, *68*, 441.

(14) (a) Sailaja, S.; Rajasekharan, M. V. *Inorg. Chem.* **2003**, *42*, 5675. (b) Kristiansson, O. *Inorg. Chem.* **2001**, *40*, 5058. (c) Singh, K.; Long, J. R.; Stavropoulos, P. *J. Am. Chem. Soc.* **1997**, *119*, 2942. (d) Pyykkö, P. *Chem. Rev.* **1997**, *97*, 597. (e) Khlobystov, A. N.; Blake, A. J.; Champness, N. R.; Lemenovskii, D. A.; Majouga, A. G.; Zyk, N. V.; Schroder, M. *Coord. Chem. Rev.* **2001**, *222*, 155.



the triflate anions and the second silver atom are considered along with the three equatorial nitrogen atoms, the geometry around each silver becomes trigonal bipyramidal. Other structural characteristics of this compound will be analyzed in a forthcoming paper, together with other compounds with similar structures that involve Ag–Ag interactions.

## Discussion

The structures described here fall within the general structural trends found with silver(I) complexes of the  $C_6H_{6-n}[CH_2OCH_2C(pz)_3]_n$  ( $n = 2, 3, 4,$  and  $6$ ) family of ligands. Specifically, the structures of compounds **1–7** are counterion and solvent dependent, as observed in all previously described cases.<sup>7</sup> Changing the counterion, especially to triflate, has a greater effect on the structures than observed previously.

The most important trend in all these structures is the overwhelming dominance of the  $\kappa^2-\kappa^1$  bonding mode of the  $[C(pz)_3]$  units in all of these ligands. In all but one of the cases reported here, **7**, this bonding mode leads to the formation of coordination polymers that we have referred to as argentachains, in which no direct Ag...Ag interaction is implied (Ag...Ag distances in the  $\kappa^2-\kappa^1$  bonding mode range from 4.12 to 5.55 Å<sup>7</sup>). In five of the cases, the argentachains are supported solely by the  $\kappa^2-\kappa^1$  bonding mode, whereas in  $\{[C_6H_5CH_2OCH_2C(pz)_3]_2Ag_3\}(OTf)_3 \cdot 0.5[(CH_3)_2CO]$ , the chains are formed, in addition, by interactions of the triflate counterion. In **7**, the  $\kappa^2-\kappa^1$  bonding mode to the same two silvers supports isolated dimers. In designing the  $C_6H_{6-n}[CH_2OCH_2C(pz)_3]_n$  family of ligands, we anticipated the formation of coordination polymers built upon the intrinsic linking of the  $[C(pz)_3]$  units in a single multitopic ligand but did not anticipate this bridging  $\kappa^2-\kappa^1$  linking feature to be so dominant. This dominance is clearly confirmed by the new structures in this work, including structures of the “first generation” HC(pz)<sub>3</sub> ligand, demonstrating that the  $\kappa^2-\kappa^1$  bonding mode, frequently leading to argentachains, is a general feature in complexes of silver(I) with ligands containing the  $[C(pz)_3]$  unit and is not specific to the “third generation,” multitopic ligands. This type of bonding has also been shown to occur for  $[HC(pz)_3Ag](NO_3)$ .<sup>16</sup> In contrast,  $\kappa^3$  bonding is the dominant coordination mode of tris(pyrazolyl)borate and ring-substituted tris(pyrazolyl)methane ligands.<sup>15</sup> For example, in our first silver(I) paper with tris(pyrazolyl)methane ligands, we used the substituted ligands HC(3,5-Me<sub>2</sub>pz)<sub>3</sub> and HC(3-Bu<sup>t</sup>pz)<sub>3</sub>.<sup>17</sup> In the structures of the silver(I) complexes of these ligands, the  $\kappa^3$  bonding mode is observed. Clearly, substitution on the pyrazolyl rings favors this type of bonding, whereas the  $[C(pz)_3]$  unit, at least in silver(I) chemistry, favors the  $\kappa^2-\kappa^1$  bonding mode.

One of the basic ideas behind this report is to determine if the removal of one or more “sidearms” from our multitopic ligands will still lead to similar covalent bonding and supramolecular structural trends with those observed previously with multitopic ligands. In general, the structures reported here have similar bonding characteristics but are much less complex, both in terms of the covalent bonding and the supramolecular structures. For example, the structure of **1** reveals a similar argentachain organization as  $\{m-C_6H_4[CH_2OCH_2C(pz)_3]_2Ag_2\}(BF_4)_2$  (**8**) (for full details see ref 7h) with different types of silver(I) centers in alternating linear and tetrahedral environments. The difference is that in the structure of **8**, in addition to the simple argentachain structure of **1**, the additional linkage provided by the bitopic ligand leads to a more complex chain of 32 atom metallomacrocycles. Also, in **8** the central arene rings were involved in  $\pi-\pi$  stacking, thus expanding the dimensionality of the supramolecular structure, whereas in compound **1** no such interaction exists.

The absence of multiple sidearms in **2·0.5[(CH<sub>3</sub>)<sub>2</sub>CO]**, when compared to  $\{p-C_6H_4[CH_2OCH_2C(pz)_3]_2Ag_2\}(OTf)_2$  (**9**), also influences the structure in that **2·0.5[(CH<sub>3</sub>)<sub>2</sub>CO]** shows unique features not encountered in other cases where the tris(pyrazolyl)methane unit was used as a donor set. The counterion was found coordinated to the silver(I) atom and also bridging two “independent”  $(L1)_2(Ag)_3$  units through covalent and secondary bonds. In the complex structure of **9**, the triflate anions are not bonded to the silver but organize the supramolecular structure into a tubular 3D arrangement (for details see ref 7i). As with **1**, no noncovalent interactions involving groups other than the triflate groups were identified in the structure of **2·0.5[(CH<sub>3</sub>)<sub>2</sub>CO]**.

With the HOCH<sub>2</sub>C(pz)<sub>3</sub> alcohol as the ligand, the structure of  $\{[HOCH_2C(pz)_3]Ag\}(BF_4) \cdot 0.5[(CH_3)_2CO]$  is also a simple covalent 1D coordination polymer, but the BF<sub>4</sub><sup>−</sup> ion organizes them in a 3D structure, as observed with complexes of this ion using the multitopic ligands. In the latter cases, the structures are more complex because of the linkages provided by the ligands. As observed with **2·0.5[(CH<sub>3</sub>)<sub>2</sub>CO]**, in the case of **4**, the triflate counterions are coordinated to half of the silver centers and also organize the normal  $\kappa^2-\kappa^1$  argentachain structure into sheets.

Upon further simplifying the ligands, that is, using HC(pz)<sub>3</sub>, two different situations were encountered. With **7**, the triflate ion coordinates to the silver centers, leading to a discrete bimetallic compound rather than argentachains. The two other compounds, **5** and **6·0.5[(CH<sub>3</sub>)<sub>2</sub>CO]**, are simple 1D coordination polymers, built up by a  $\kappa^2-\kappa^1$  bonding mode of the tris(pyrazolyl)methane ligands, although in the structure of **6·0.5[(CH<sub>3</sub>)<sub>2</sub>CO]** the BF<sub>4</sub><sup>−</sup> ion organizes the polymers into corrugated sheets. In striking similarity with  $\{p-C_6H_4[CH_2OCH_2C(pz)_3]_2Ag_2CH_3CN\}(BF_4)_2 \cdot (C_4H_{10}O)$ ,<sup>7i</sup> **5** also contains two different types of silvers; one Ag atom is four coordinate, bonded by three pyrazolyl rings with the fourth site occupied by an acetonitrile molecule, and one Ag atom is only three coordinate. In addition, in both structures, the latter Ag atom makes a  $\pi$ -contact with a pyrazolyl ring, as pictured in Figure 9.

(15) (a) Trofimenko, S. *Scorpionates: The Coordination Chemistry of Polypyrazolylborate Ligands*; Imperial College Press: London, 1999. (b) Pettinari, C.; Pettinari, R. *Coord. Chem. Rev.* **2005**, *249*, 525.

(16) Cingolani, A.; Effendy, G.; Martini, D.; Pellei, M.; Pettinari, C.; Skelton, B. W.; White, A. H. *Inorg. Chem. Acta* **2002**, *328*, 87.

(17) Reger, D. L.; Collins, J. E.; Rheingold, A. L.; Liable-Sands, L. M.; Yap, G. P. A. *Organometallics* **1997**, *16*, 349.

The PF<sub>6</sub><sup>-</sup> counterion in **6·0.5**[(CH<sub>3</sub>)<sub>2</sub>CO] has no organizational function. Its structure is a simple 1D coordination polymer, with no remarkable supramolecular structural characteristics. This result is consistent with our previous findings,<sup>7i</sup> where the PF<sub>6</sub><sup>-</sup> anion, when present, was not involved in a supramolecular organization of the covalent networks.

On the basis of our results reported here, we can clearly state that the presence of the rigid core of the multitopic ligands contributes to the highly organized supramolecular structures. Further, the presence of multiple [C(pz)<sub>3</sub>]-containing sidearms grafted onto the central arene ring is important for this functional group to show supramolecular associations, as well as to control the orientation around the central arene core. For example, when comparing compound **1** with **8**, we found no  $\pi$ - $\pi$  stacking in the former, while strong  $\pi$ - $\pi$  stacking interactions in the latter led to an increased dimensionality of the crystal structure. It is well known that substituents perturb the uniform charge distribution in aromatic rings (which, in our case, is the central arene core), causing partial atomic charges and a permanent dipole, which introduce electrostatic dipole-dipole and dipole-induced dipole forces that are responsible for the increased stability of  $\pi$ -stacked species.

The flexible ether linkage role is also crucial. It is the flexibility of the ether linkage that allows the anions to organize the structures observed in our studies; rigid ligands would have to be perfectly tailored to allow such structures, and their inherent rigidity would restrict the influence of the anions in the final structures. Therefore, ligands based on tris(pyrazolyl)methane units linked with flexible organic spacers are ideal candidates for studying the self-assembly process in its entirety and especially the interplay between different types of noncovalent interaction.

## Conclusion

The major structural characteristic of all the complexes that contain the [C(pz)<sub>3</sub>] unit with silver(I) as the metal is that all of these ligands strongly favor the  $\kappa^2$ - $\kappa^1$  bonding mode. Also important is the number of the donor units within the ligand and their relative position with respect to each other. The crystal packing is influenced by a combination of noncovalent interactions. The two opposed structural characteristics built into the C<sub>6</sub>H<sub>6-n</sub>[CH<sub>2</sub>OCH<sub>2</sub>C(pz)<sub>3</sub>]<sub>n</sub> family of ligands (rigid groups and flexible linkers) are complementary; while the rigid groups definitely support special organizational features within the structures, the flexible linkers allow *all* these features to manifest themselves in a cumulative and complementary manner.

The counterions also impose changes in the overall structures of the crystalline solids; these differences are much greater with the simple ligands reported here and when the material is crystallized from a noncoordinating solvent. The crystallization of these systems from weakly coordinating solvents allows the weak forces to dominate the structures; the three coordinate silver centers appear to be more flexible in accommodating particular structures than the four-coordinate silvers in the complexes crystallized from aceto-

nitrile. We have also shown that, although the structures reported here are different, several important patterns can be found that can be transferred from one case to another. Therefore, this strategy for the assembly of covalent networks based on semirigid ligands completes the gap between strategies based on rigid or completely flexible ligands.

## Experimental Section

**General Procedure.** All operations were carried out under a nitrogen atmosphere using standard Schlenk techniques and a Vacuum Atmospheres HE-493 drybox. All solvents were dried and distilled prior to use following standard techniques. The <sup>1</sup>H NMR spectra were recorded on a Varian AM300 spectrometer using a broad-band probe. Proton chemical shifts are reported in ppm vs internal Me<sub>4</sub>Si. Elemental analyses were performed by Robertson Microlit Laboratories (Madison, NJ). Tris(pyrazolyl)methane, HC(pz)<sub>3</sub> (**L3**), and tris-2,2,2-(1-pyrazolyl)ethanol, HOCH<sub>2</sub>C(pz)<sub>3</sub> (**L2**), were prepared following literature methods.<sup>10</sup> The starting materials benzyl bromide, silver tetrafluoroborate, silver hexafluorophosphate, and silver triflate were obtained from commercial sources (Aldrich) and used as received.

**Synthesis of C<sub>6</sub>H<sub>5</sub>[CH<sub>2</sub>OCH<sub>2</sub>C(pz)<sub>3</sub>] (**L1**).** Benzyl bromide (1.71 g, 10 mmol) and tris-2,2,2-(1-pyrazolyl)ethanol, HOCH<sub>2</sub>C(pz)<sub>3</sub> (2.44 g, 10 mmol), were dissolved in dry THF (75 mL). This solution was added dropwise to a suspension of NaH (1.0 g) in dry THF (100 mL) under an inert atmosphere. The mixture was stirred under reflux for 12 h and then allowed to cool at room temperature. To this solution enough water (250 mL) was added dropwise to consume the excess NaH and dissolve the resulting NaBr and NaOH. The THF-water mixture was extracted with ethyl ether (4 × 100 mL), and the combined organic extracts were washed with 100 mL of saturated NaHCO<sub>3</sub> solution, with 100 mL of saturated NaCl solution, and finally with 100 mL of water. The organic layer was dried over anhydrous Na<sub>2</sub>SO<sub>4</sub> and filtered, and the solvent removed under vacuum to afford the desired compound as a white powder (3.11 g, 93%); <sup>1</sup>H NMR (acetone-*d*<sub>6</sub>):  $\delta$  7.60, 7.50 (d, d, *J* = 1.5, 2.4 Hz, 3,3H, 3,5-H *pz*), 7.29 (m, 5H, C<sub>6</sub>H<sub>5</sub>), 6.35 (dd, 3H, *J* = 1.5, *J* = 2.4 Hz, 4-H *pz*), 5.13 (s, 2H, OCH<sub>2</sub>C(pz)<sub>3</sub>), 4.57 (s, 2H, OCH<sub>2</sub>Ph); ES<sup>+</sup>/MS for [C<sub>18</sub>H<sub>19</sub>N<sub>6</sub>O]<sup>+</sup>: Calcd 335.1620; Found 335.1621.

**Synthesis of {[C<sub>6</sub>H<sub>5</sub>CH<sub>2</sub>OCH<sub>2</sub>C(pz)<sub>3</sub>]Ag}(BF<sub>4</sub>) (**1**).** A THF (20 mL) solution of **L1** (0.334 g, 1 mmol) was added dropwise to a solution of AgBF<sub>4</sub> (0.194 g, 1.00 mmol) in dry THF (20 mL) under an inert atmosphere. A white precipitate appeared as the mixture was stirred for 2 h. The THF was removed by cannula filtration, and the white precipitate washed with THF (2 × 10 mL) and then vacuum-dried to afford 0.492 g (93%) of solid identified as {[C<sub>6</sub>H<sub>5</sub>CH<sub>2</sub>OCH<sub>2</sub>C(pz)<sub>3</sub>]Ag}(BF<sub>4</sub>). Crystallization of this compound from acetone afforded {[C<sub>6</sub>H<sub>5</sub>CH<sub>2</sub>OCH<sub>2</sub>C(pz)<sub>3</sub>]Ag}(BF<sub>4</sub>). <sup>1</sup>H NMR (acetone-*d*<sub>6</sub>):  $\delta$  7.91, 7.77 (d, d, *J* = 1.5, 2.4 Hz, 3,3H, 3,5-H *pz*), 7.32 (m, 5H, C<sub>6</sub>H<sub>5</sub>), 6.52 (dd, 3H, *J* = 1.5, *J* = 2.4 Hz, 4-H *pz*), 5.17 (s, 2H, OCH<sub>2</sub>C(pz)<sub>3</sub>), 4.65 (s, 2H, OCH<sub>2</sub>Ph); Calcd for C<sub>18</sub>H<sub>18</sub>AgBF<sub>4</sub>N<sub>6</sub>O: C, 40.86; H, 3.43; N, 15.89; Found C, 40.81; H, 2.99, N, 15.50; ES<sup>+</sup>/MS: Calcd for [C<sub>6</sub>H<sub>5</sub>CH<sub>2</sub>OCH<sub>2</sub>C(pz)<sub>3</sub>]Ag<sup>+</sup> *m/z* 441.0593, Found 441.0584.

**Synthesis of {[C<sub>6</sub>H<sub>5</sub>CH<sub>2</sub>OCH<sub>2</sub>C(pz)<sub>3</sub>]Ag}(OTf) (**2**).** This compound was synthesized as above for **1** using AgOTf (0.256 g, 1.00 mmol) to afford 0.510 g (86%) of solid identified as {[C<sub>6</sub>H<sub>5</sub>CH<sub>2</sub>OCH<sub>2</sub>C(pz)<sub>3</sub>]Ag}(OTf). Crystallization of this compound from acetone afforded **2·0.5**[(CH<sub>3</sub>)<sub>2</sub>CO]. <sup>1</sup>H NMR (acetone-*d*<sub>6</sub>):  $\delta$  7.90, 7.76 (d, d, *J* = 1.5, 2.4 Hz, 3,3H, 3,5-H *pz*), 7.32 (m, 5H, C<sub>6</sub>H<sub>5</sub>), 6.52 (dd, 3H, *J* = 1.5, *J* = 2.4 Hz, 4-H *pz*), 5.17 (s, 2H, OCH<sub>2</sub>C-

**Table 1.** Selected Crystal and Structure Refinement Data

	1	2·0.5[(CH <sub>3</sub> ) <sub>2</sub> CO]	3·0.5[(CH <sub>3</sub> ) <sub>2</sub> CO]	4
formula	C <sub>18</sub> H <sub>18</sub> AgBF <sub>4</sub> N <sub>6</sub> O	C <sub>40.50</sub> H <sub>39</sub> Ag <sub>3</sub> F <sub>9</sub> N <sub>12</sub> O <sub>11.50</sub> S <sub>3</sub>	C <sub>12.50</sub> H <sub>15</sub> AgBF <sub>4</sub> N <sub>6</sub> O <sub>1.50</sub>	C <sub>12</sub> H <sub>12</sub> AgF <sub>3</sub> N <sub>6</sub> O <sub>4</sub> S
fw, g mol <sup>-1</sup>	529.06	1468.63	467.98	501.21
cryst syst	triclinic	monoclinic	monoclinic	orthorhombic
space group	<i>P</i> $\bar{1}$	<i>P</i> 2 <sub>1</sub> / <i>c</i>	<i>P</i> 2 <sub>1</sub> / <i>n</i>	<i>P</i> <i>n</i> <i>m</i>
<i>T</i> (K)	190(2)	293(2)	190(2)	150(2)
<i>a</i> , Å	10.8577(8)	12.2301(18)	9.0888(13)	13.6420(7)
<i>b</i> , Å	20.0205(15)	13.1990(19)	22.974(3)	13.9842(7)
<i>c</i> , Å	21.8994(16)	32.933(5)	16.479(2)	17.9820(9)
$\alpha$ , deg	116.6500(10)	90	90	90
$\beta$ , deg	93.116(2)	100.761(3)	92.219(3)	90
$\gamma$ , deg	102.1530(10)	90	90	90
<i>V</i> , Å <sup>3</sup>	4098.6(5)	5222.7(13)	3438.2(8)	3430.5(3)
<i>Z</i>	8	4	8	8
R1 <i>I</i> > 2 $\sigma$ ( <i>I</i> )	0.0412	0.0489	0.0468	0.0433
wR2 <i>I</i> > 2 $\sigma$ ( <i>I</i> )	0.0872	0.1110	0.1283	0.0921

	5	6·0.5[(CH <sub>3</sub> ) <sub>2</sub> CO]	7
formula	C <sub>22</sub> H <sub>23</sub> Ag <sub>2</sub> B <sub>2</sub> F <sub>8</sub> N <sub>13</sub>	C <sub>11.50</sub> H <sub>13</sub> AgF <sub>6</sub> N <sub>6</sub> O <sub>0.50</sub> P	C <sub>22</sub> H <sub>20</sub> Ag <sub>2</sub> F <sub>6</sub> N <sub>12</sub> O <sub>6</sub> S <sub>2</sub>
fw, g mol <sup>-1</sup>	858.89	496.12	942.36
cryst syst	monoclinic	monoclinic	triclinic
space group	<i>P</i> 2 <sub>1</sub> / <i>c</i>	<i>P</i> 2 <sub>1</sub> / <i>c</i>	<i>P</i> $\bar{1}$
<i>T</i> (K)	150(2)	190(2)	150(2)
<i>a</i> , Å	10.0218(6)	11.6571(8)	8.6922(6)
<i>b</i> , Å	12.6040(7)	13.5851(9)	9.4966(7)
<i>c</i> , Å	23.8071(13)	10.7084(7)	10.3316(8)
$\alpha$ , deg	90	90	71.5870(10)
$\beta$ , deg	95.0650(10)	97.6620(10)	68.4530(10)
$\gamma$ , deg	90	90	81.8470(10)
<i>V</i> , Å <sup>3</sup>	2995.4(3)	1680.67(19)	752.30(10)
<i>Z</i>	4	4	1
R1 <i>I</i> > 2 $\sigma$ ( <i>I</i> )	0.0330	0.0596	0.0247
wR2 <i>I</i> > 2 $\sigma$ ( <i>I</i> )	0.0766	0.1621	0.0600

(pz)<sub>3</sub>, 4.65 (s, 2H, OCH<sub>2</sub>Ph); Calcd For C<sub>19</sub>H<sub>18</sub>AgF<sub>3</sub>N<sub>6</sub>O<sub>4</sub>S: C, 38.59; H, 3.07; N, 14.21; Found C, 38.51; H, 3.02, N, 14.53.

**Synthesis of {[HOCH<sub>2</sub>C(pz)<sub>3</sub>]Ag}(BF<sub>4</sub>) (3).** A THF (20 mL) solution of **L2** (0.244 g, 1 mmol) was added dropwise to a solution of AgBF<sub>4</sub> (0.194 g, 1.00 mmol) in dry THF (20 mL) under an inert atmosphere. A white precipitate appeared as the mixture was stirred for 2 h. The THF was removed by cannula filtration, and the white precipitate washed with THF (2 × 10 mL) and then vacuum-dried to afford 0.401 g (91%) of solid identified as {[HOCH<sub>2</sub>C(pz)<sub>3</sub>]Ag}-(BF<sub>4</sub>). Crystallization of this compound from acetone afforded {[HOCH<sub>2</sub>C(pz)<sub>3</sub>]Ag}·0.5[(CH<sub>3</sub>)<sub>2</sub>CO]. <sup>1</sup>H NMR (acetone-*d*<sub>6</sub>):  $\delta$  7.91, 7.77 (d, d, *J* = 1.5, 2.4 Hz, 3,3H, 3,5-H *pz*), 7.32 (m, 5H, C<sub>6</sub>H<sub>5</sub>), 6.52 (dd, 3H, *J* = 1.5, *J* = 2.4 Hz, 4-H *pz*), 5.17 (s, 2H, OCH<sub>2</sub>C(pz)<sub>3</sub>), 4.65 (s, 2H, OCH<sub>2</sub>Ph); Calcd for C<sub>11</sub>H<sub>12</sub>AgBF<sub>4</sub>N<sub>6</sub>O: C, 30.10; H, 2.76; N, 19.15; Found C, 30.57; H, 2.99, N, 19.72.

**Synthesis of {[HOCH<sub>2</sub>C(pz)<sub>3</sub>]Ag}(OTf) (4).** This compound was synthesized as above, using AgOTf (0.256 g, 1.00 mmol), to afford 0.432 g (86%) of solid identified as {[HOCH<sub>2</sub>C(pz)<sub>3</sub>]Ag}-(OTf). <sup>1</sup>H NMR (acetone-*d*<sub>6</sub>):  $\delta$  7.91, 7.77 (d, d, *J* = 1.5, 2.4 Hz, 3,3H, 3,5-H *pz*), 7.32 (m, 5H, C<sub>6</sub>H<sub>5</sub>), 6.52 (dd, 3H, *J* = 1.5, *J* = 2.4 Hz, 4-H *pz*), 5.17 (s, 2H, OCH<sub>2</sub>C(pz)<sub>3</sub>), 4.65 (s, 2H, OCH<sub>2</sub>Ph); Calcd for C<sub>12</sub>H<sub>12</sub>AgF<sub>3</sub>N<sub>6</sub>O<sub>4</sub>S: C, 28.76; H, 2.41; N, 16.77; Found C, 28.32; H, 2.83, N, 17.14.

**Synthesis of {[HC(pz)<sub>3</sub>]Ag}(BF<sub>4</sub>) (5).** A THF (20 mL) solution of **L3** (0.214 g, 1 mmol) was added dropwise to a solution of AgBF<sub>4</sub> (0.194 g, 1.00 mmol) in dry THF (20 mL) under an inert atmosphere. A white precipitate appeared as the mixture was stirred for 2 h. The THF was removed by cannula filtration, and the white precipitate was washed with thf (2 × 10 mL) and then vacuum-dried to afford 0.362 g (88%) of solid identified as {[HC(pz)<sub>3</sub>]Ag}-(BF<sub>4</sub>). Crystallization of this compound from acetonitrile afforded **5**. <sup>1</sup>H NMR (acetone-*d*<sub>6</sub>):  $\delta$  9.29 (s, 1H, HC(pz)<sub>3</sub>), 8.25, 7.83 (s, s,

3,3H, 3,5-H *pz*), 6.54 (s, 3H, 4-H *pz*); Calcd for C<sub>10</sub>H<sub>10</sub>AgBF<sub>4</sub>N<sub>6</sub>: C, 29.37; H, 2.47; N, 20.55; Found C, 28.98; H, 2.89, N, 19.99.

**Synthesis of {[HC(pz)<sub>3</sub>]Ag}(PF<sub>6</sub>) (6).** This compound was synthesized as above, using AgPF<sub>6</sub> (0.252 g, 1.00 mmol), to afford 0.392 g (83%) of solid identified as {[HC(pz)<sub>3</sub>]Ag}(PF<sub>6</sub>). Crystallization of this compound from acetone afforded {[HC(pz)<sub>3</sub>]Ag}-(PF<sub>6</sub>)·0.5[(CH<sub>3</sub>)<sub>2</sub>CO]. <sup>1</sup>H NMR (acetone-*d*<sub>6</sub>):  $\delta$  9.29 (s, 1H, HC(pz)<sub>3</sub>), 8.24, 7.86 (s, s, 3,3H, 3,5-H *pz*), 6.54 (s, 3H, 4-H *pz*); Calcd for C<sub>10</sub>H<sub>10</sub>AgF<sub>6</sub>N<sub>6</sub>P: C, 25.72; H, 2.16; Found C, 24.73; H, 2.18.

**Synthesis of {[HC(pz)<sub>3</sub>]Ag}(OTf) (7).** This compound was synthesized as above, using AgOTf (0.256 g, 1.00 mmol), to afford 0.392 g (83%) of solid identified as {[HC(pz)<sub>3</sub>]Ag}(OTf). <sup>1</sup>H NMR (acetone-*d*<sub>6</sub>):  $\delta$  9.30 (s, 1H, HC(pz)<sub>3</sub>), 8.24, 7.85 (s, s, 3,3H, 3,5-H *pz*), 6.54 (s, 3H, 4-H *pz*); Calcd for C<sub>11</sub>H<sub>10</sub>AgF<sub>3</sub>N<sub>6</sub>O<sub>3</sub>S: C, 28.04; H, 2.14; N, 17.84; Found C, 28.12; H, 2.53, N, 17.44.

**Crystallography.** All crystals were mounted on thin glass fibers with inert oil. After preliminary crystal quality, symmetry, and unit cell parameter determination, a full sphere (**1**, **5**, **6·0.5[(CH<sub>3</sub>)<sub>2</sub>CO]** or a hemisphere (**2·0.5[(CH<sub>3</sub>)<sub>2</sub>CO]**, **3·0.5[(CH<sub>3</sub>)<sub>2</sub>CO]**, **4**, **7**) of X-ray intensity data was collected on a Bruker SMART APEX CCD-based diffractometer (Mo K $\alpha$  radiation,  $\lambda$  = 0.71073 Å).<sup>18</sup> Raw area detector data frame integration and Lorentz/polarization corrections were carried out with SAINT+.<sup>18</sup> Final unit cell parameters are based on the least-squares refinement of all reflections with *I* > 5 $\sigma$ (*I*) from each data set. Direct methods structure solution, difference Fourier calculations, and full-matrix least-squares refinement against *F*<sup>2</sup> were performed with SHELXTL

(18) SMART Version 5.624, SAINT+ Version 6.02a, and SADABS; Bruker Analytical X-ray Systems, Inc.: Madison, WI, 1998.

(19) Sheldrick, G. M. SHELXTL Version 5.1; Bruker Analytical X-ray Systems, Inc.: Madison, WI, 1997.



*Crystal Engineering Based on Tris(pyrazolyl)methane Ligands*

for all structures.<sup>19</sup> Selected crystal and structure refinement data can be found in Table 1.

**Acknowledgment.** The financial support from the National Science Foundation (CHE-0414239) is greatly appreciated.

**Supporting Information Available:** X-ray crystallographic files in CIF format and details of crystal structure determination for all compounds. This material is available free of charge via the Internet at <http://pubs.acs.org>.

IC0606936